doi:10.2533/chimia.2025.232 Chimia 79 (2025) 232–236

Towards Biocompatible Cellulose Nanofiber Sponges with Tailored Pore Geometries

Flavio Augusto von Philipsborn[§a,b] and Christian Adlhart*[a]

[§]SCS-dsm-firmenich Award for the best poster presentation in Material Chemistry

Abstract: Cellulose nanofiber (CNF) sponges or CNF aerogels are promising biocompatible materials with applications ranging from biomedicine to environmental remediation. The highly porous architecture of these sponges – which is crucial for their functionality – is significantly influenced by the freezing step during fabrication. This review explores the critical role of freezing techniques in tailoring pore geometry and, consequently, the macroscopic properties of CNF sponges. We discuss conventional directional freezing methods and their limitations, highlighting the advantages of dynamic freezing for achieving isotropic pore structures. Furthermore, we examine various crosslinking strategies to enhance the stability and mechanical properties of CNF sponges. Finally, we present recent findings from our laboratory demonstrating the successful fabrication of biocompatible and crosslinked CNF sponges with tailored pore geometries using a dynamic freezing approach.

Keywords: Biocompatible · CNF aerogels · CNF sponges · Crosslinking · Freeze-drying · Pore geometry

Flavio von Philipsborn completed his apprenticeship at the Zurich University of Applied Sciences (ZHAW), where he graduated with a BSc in Chemistry in 2023. Currently, he is pursuing his Master's studies at the University of Zurich, where he is investigating the dynamics of soluble GPCR analogues by BioNMR under the guidance of Prof. Dr. Oliver Zerbe.

1. Introduction

The growing demand for sustainable materials derived from renewable resources has fueled intense research into cellulose nanofibers (CNF). As the most abundant biopolymer on earth, cellulose offers a compelling platform for developing advanced materials with exceptional properties.[1,2] Among these, CNF sponges, also known as CNF aerogels, have emerged as a promising class of three-dimensional nanomaterials. These lightweight, highly porous structures possess a high specific surface area and a rich density of functional groups making them suitable for a wide range of promising applications.[1,3] They can be used for heat and sound insulation,[4] as adsorption and absorption agents for various pollutants,[5,6] as catalyst supports,[7] for energy storage and energy conversion[8] or in the broad field of biomedicine.[9]

In nature, cellulose is found in the cell walls of plants[1] and it is also used by some bacteria as a protective envelope around their cells.[10] Cellulose in plants exhibits a hierarchical structure ranging from the meter to the nanometer scale (Fig. 1a). Macroscopic cellulose fibers are composed of micro fibrils, which can be further converted into CNFs.[11] The isolation of CNF from biomass proceeds *via* two major steps: first native cellulose fibers are pre-treated using strong acidic conditions for hydrolysis to occur. Second, CNFs are obtained by applying strong shear forces using high pressure homogenizers.[12]

CNF sponges are typically fabricated through a multi-step process (Fig. 1b) involving CNF dispersion (1), freezing (2), lyophilization (freeze-drying) (3), and crosslinking (4).

The freezing step is particularly critical as it dictates the final architecture of the sponges.[13,14] Conventional freezing techniques are static and often lead to anisotropic pore structures, limiting the performance of the sponges in certain applications. To address this, innovative techniques such as dynamic freezing, inspired by ice cream manufacturing, have been introduced to achieve isotropic pore structures.[15] Alternatively, isotropy is achieved by replacing lyophilization by supercritical drying.[16] This review provides a comprehensive overview of CNF sponge fabrication, with a particular emphasis on the influence of freezing techniques and crosslinking strategies on pore geometry and macroscopic properties. We also present recent advances from our laboratory, where we employed a dynamic freezing approach to synthesize biocompatible and crosslinked CNF sponges.

2. Synthesis of CNF Sponges

The fabrication of CNF sponges involves four fundamental steps (Fig. 1b): dispersing the CNF in a suitable liquid (1), freezing the dispersion (2), lyophilizing the frozen structure to remove the dispersing liquid (3), and crosslinking the resulting sponge to enhance its stability (4).[17] Crosslinking is usually thermally initiated using crosslinking agents that have been added before freezing.

2.1 *Dispersing*

The CNF building blocks are first homogenized in a dispersing liquid by applying shear forces, which cause the fibers to un-

*Correspondence: Prof. Dr. C. Adlhart, E-mail: christian.adlhart@zhaw.ch
[a]Institute of Chemistry and Biotechnology, Zurich University of Applied Sciences ZHAW, CH-8820 Wädenswil, Switzerland; [b]University of Zurich, Department of Chemistry, CH-8057 Zurich, Switzerland.

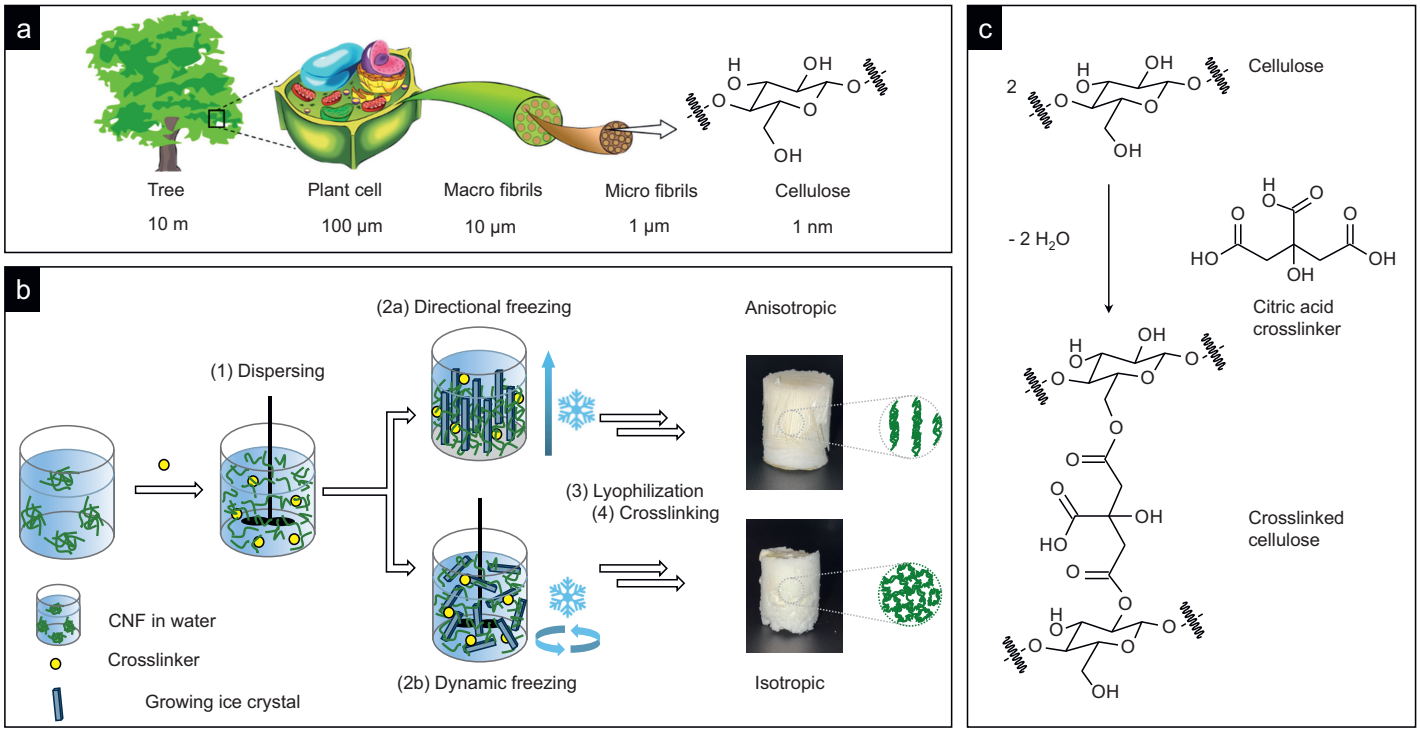

Fig. 1. (a) Hierarchical structure of cellulose, adapted from ref. [2]; (b) fabrication steps for the synthesis of CNF sponges; (c) reaction scheme for the crosslinking of cellulose with citric acid.

tangle and break into smaller pieces. The choice of the dispersing liquid depends on the fiber material. The fibers must be wetted but not dissolved.[17] In the case of cellulose, water is commonly used. It is suitable due to its high polarity and ability to form hydrogen bonds with CNFs.[18,19]

CNF concentrations between 1 and 2 wt% are commonly reported as optimal.[19] In the following processing step the nanofiber dispersion is transferred into a mold and frozen. The selected dispersing liquid as well as the fiber concentration influence the subsequent freezing process.[17]

2.2 *Freezing*

The freezing step is pivotal in determining the porous architecture of the CNF sponge. During freezing, ice crystals grow within the CNF dispersion, and the CNF building blocks become entrapped between these crystals.[19,20] The morphology of the ice crystals, influenced by the freezing technique and the dispersing liquid, determines the final pore structure.[17] While water leads to a lamellar pore morphology, other dispersing liquids give rise to honeycomb[3] or cubic structures.[17]

Table 1 gives an overview of freezing techniques for the synthesis of CNF sponges and their impact on the macroscopic properties of the sponges. Traditional freezing methods, such as unidirectional and bidirectional freezing, often result in anisotropic, lamellar pore structures. Based on the principle that ice crystal growth follows the direction of the temperature gradient, ice crystals nucleate at the cooled bottom of a freezing mold from which they grow to the top. For bidirectional freezing the process is initiated from two cooled walls of the molds.[15] Multidirectional freezing can improve pore homogeneity, however it still leads to predominantly lamellar structures due to the inherent freezing nature of water. Furthermore, these static freezing techniques can cause CNF segregation, leading to inhomogeneities within the sponge.

The freezing rate, controlled by the temperature gradient, also significantly affects pore size.[13,14,19] Typical methods include simply placing the mold in a freezer (*e.g.* –20 °C or –80 °C), freezing media with defined temperature,[21] or contact materials with high thermal conductivity.[19] Rapid freezing, such as shock-freezing with liquid nitrogen, can preserve the isotropic arrangement of CNFs to a greater extent.[14] However, this method is limited to small sponge sizes due to thermal stress and limited conductivity.[22,23]

Dynamic freezing offers a promising alternative to overcome the limitations of conventional methods. By simultaneously stirring and freezing the dispersion, dynamic freezing promotes the formation of isotropic pore structures with enhanced homogeneity based on the elimination of the temperature gradient and the formation of smaller ice crystals.[15,24]

This approach, inspired by ice cream manufacturing, allows greater control over pore geometry, if the structure and texture of the frozen dispersion can be preserved during lyophilization.[24]

Table 1. Freezing strategies applied for the fabrication of CNF sponges.

Freezing strategy	Pore geometry	Macroscopic properties	Ref.
Unidirectional	Anisotropic	Reduced thermal conductivity, improved elasticity, high air permeability	[25] [26] [14]
Bidirectional	Anisotropic, highly ordered	Enhanced mechanical stability	[27]
Multidirectional	Isotropic, homogeneous	Improved thermal insulation	[28]
Dynamic freezing	Isotropic, globular pores	Enhanced mechanical properties	[21] [29]

2.3 *Lyophilization*

Once the nanofiber dispersion is fully frozen, the next step involves the removal of the frozen pore fluid. Here it is important to preserve the structural properties and to minimize structural degradation during sublimation. Lyophilization is a gentle process, that preserves the porous structure formed during freezing.[30]

2.4 *Crosslinking*

The lyophilized CNF sponges are often fragile due to weak non-covalent inter-fiber interactions. Thus, it is vital to reinforce the intersection points of the fibers.[3] This can be achieved through chemical crosslinking, which involves the formation of covalent bonds between CNFs using crosslinking agents or physical crosslinking,[30,31] *e.g.* through thermal phase transition[16,32] or solvent vapor welding.[33] Further methods include ions for strong electrostatic interactions, enzymes or radiation to induce chemical bonds between the polymer fibers.[3,30,31]

Table 2 displays crosslinking agents and reaction conditions to reinforce CNF sponges for their final applications, *e.g.* in aqueous medium.[32] Given the OH functional groups of cellulose, polycarboxylic acids or acid anhydrides are widely used to form crosslinks through esterification. Citric acid is particularly interesting due to its antibacterial properties, biodegradability and non-toxicity to cells.[34] Polyethyleneimine (PEI) is a frequently encountered modifier with high water solubility, good environmental compatibility and a rich density of reactive amino groups. CNF crosslinking is achieved by combining PEI with GPTMS. PEI modified CNF sponges are used as adsorption agents, sensors or in bioengineering applications.[36] Further crosslinking agents are epichlorohydrin and glutaraldehyde. However, concerns like cytotoxicity in the case of glutaraldehyde or insufficient mechanical stability have limited the use of these crosslinkers.[31]

3. Recent Advances

In our work, we investigated the influence of different freezing techniques, including dynamic freezing, on the properties of crosslinked (citric acid or PEI/GPTMS) CNF sponges (Fig. 2a). We fabricated sponges with varying pore geometries and bulk densities from 14 to 61 mg cm^{-3}, achieving porosities of up to 99%. Static unidirectional freezing led to lamellar channels of different widths: shock-freezing at –196 °C resulted in significantly smaller channels (51.3 µm) than freezing at –20 °C (392 µm). In contrast, dynamic freezing resulted in an isotropic pore structure with globular pores (103 µm). Independent from the freezing technique our sponges displayed excellent elasticity and water stability. Crosslinking proved to be very effective in enhancing elasticity and water stability.

Compression curves of the CNF sponges show linear elasticity at low stress ($\varepsilon < 10\%$) followed by a long collapse plateau transitioning into a densification regime with steeply rising stress, as known for foams.[40] Our sponges were able to recover to their original height even after 80% compression (Fig. 2b). Youngs moduli of the CNF sponges were calculated from the slope in the linear regime (15% to 20%) resulting in values ranging from 13.62 ± 0.45 kPa (–196 °C, citric acid) to 70.81 ± 4.69 kPa (dynamic, PEI/GPTMS). The Youngs moduli became smaller after crosslinking, indicating an enhanced elasticity. With respect to the freezing method, the Youngs moduli were smallest for shock-freezing.

As for water stability, our sponges maintained their full structural integrity for 48 h. We also tested our sponges for their ability to let air through. This property is fundamental with respect to their use as filters.

Fig. 2c shows the measured air face velocity, v_{air}, plotted against the pressure drop Δp together with a 2nd order polynomial fit. Air permeability depends on pore size and geometry, with larger pores allowing increased airflow. The permeability, K_{air}, was calculated according to the Hagen-Poiseuille equation for compressible fluids through porous materials. We obtained values of 0.28×10^{-10} m^2 for unidirectional freezing at –196 °C, 0.48×10^{-10} m^2 for dynamic freezing and 3.23×10^{-10} m^2 for sponges produced *via* unidirectional freezing at –20 °C. The observed permeabilities are comparable with those from previous studies.[14] With respect to the application of CNF sponges as air filters, such high air permeabilities are crucial, together with their high filtration efficiency.[14,41,42]

4. Conclusions

CNF sponges are versatile bio-based materials with a wide range of potential applications. The ability to tailor their pore structure through controlled freezing techniques opens up exciting possibilities for optimizing their performance in specific applications. Dynamic freezing has emerged as a promising approach for fabricating CNF sponges with isotropic pore structures and enhanced properties. Our research demonstrates the feasibility of producing biocompatible and crosslinked CNF sponges with tailored pore geometries using various freezing techniques. These findings pave the way for the development of advanced CNF-based materials for diverse applications in fields such as water purification, air filtration, and biomedicine.

Table 2. Examples of chemical crosslinking agents used for CNF sponges. Crosslinking is either performed prior or after lyophilization (freeze-drying).

Crosslinker	Fiber material	Reaction conditions	Application / property	Ref.
Citric acid	CNF/PLA[a]	Post FD[g], 140 °C, 2 h	Biomineralization	[9]
	TOCNF[b]	Pre FD, 80 °C, 20 min	Antibacterial effects	[34]
BTCA[c]	TOCNF	Post FD, 170 °C, 3 min	Enhanced elasticity	[35]
PEI[d] / GPTMS[e]	CNF	Pre FD, rt, 2.5 h Pre & post FD, rt, 2.5 h, 110 °C, 30 min	Cu^{2+} / microplastic removal Flame retardant	[6,36] [37]
Diisocyanate	CNF	Pre FD, rt, 48 h	Water purification ($CHCl_3$)	[38]
Epichlorohydrin	MC[f]	Pre FD, 50 °C, 4 h	Energy storage	[39]
Glutaraldehyde	CNF	Post FD, rt, 1 h	Catalyst support for the reduction of 4-nitrophenol	[7]

[a]polylactide (PLA); [b]TEMPO-oxidized CNF (TOCNF); [c]butane-1,2,3,4-tetracarboxylic acid (BTCA); [d]polyethyleneimine (PEI); [e](3-glycidoxypropyl)trimethoxysilane (GPTMS); [f]methyl cellulose (MC); [g]freeze-drying (FD).

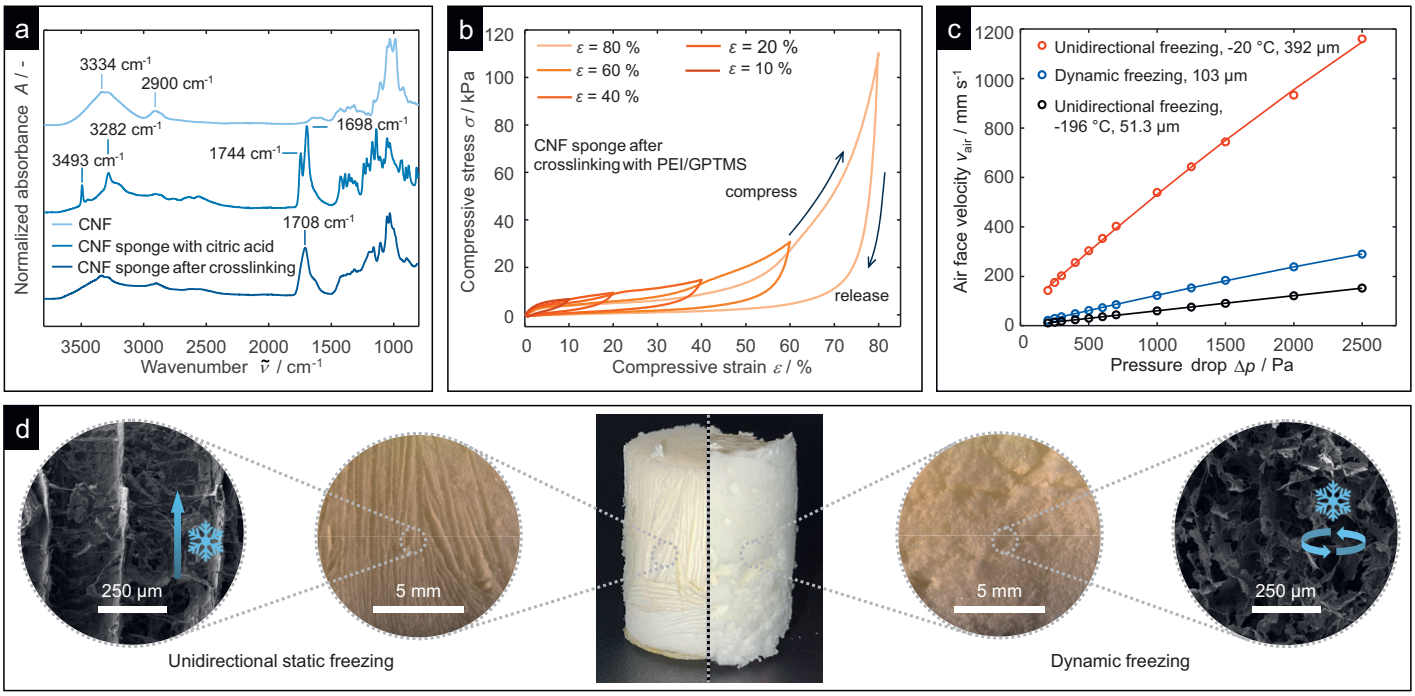

Fig. 2. Characterization of CNF sponges: (a) FT-IR spectra showing the successful crosslinking with citric acid; (b) stress-strain curves (after PEI/GPTMS crosslinking, frozen at -196 °C); (c) air permeability; and (d) pore geometry of unidirectionally and dynamically frozen CNF sponges.

Acknowledgements

F. v. Ph. thanks DSM and the Swiss Chemical Society for the SCS-dsm-firmenich poster award in Material Chemistry.

Received: January 31, 2025

[1] C. Prasad, S.-G. Jeong, J. S. Won, S. Ramanjaneyulu, S. Sangaraju, N. Kerru, H. Y. Choi, *Int. J. Biol. Macromol.* **2024**, *261,* 129460, https://doi.org/10.1016/j.ijbiomac.2024.129460.

[2] D. Miyashiro, R. Hamano, K. Umemura, *Nanomaterials* **2020**, *10*, 186, https://doi.org/10.3390/nano10020186.

[3] M. Dilamian, M. Joghataei, Z. Ashrafi, C. Bohr, S. Mathur, H. Maleki, *Appl. Mater. Today* **2021**, *22*, 100964, https://doi.org/10.1016/j.apmt.2021.100964.

[4] L. Cao, Q. Fu, Y. Si, B. Ding, J. Yu, *Compos. Commun.* **2018**, *10,* 25, https://doi.org/10.1016/j.coco.2018.05.001.

[5] M. Dilamian, B. Noroozi, *Carbohydr. Polym.* **2021**, *251,* 117016, https://doi.org/10.1016/j.carbpol.2020.117016.

[6] C. Tang, P. Brodie, Y. Li, N. J. Grishkewich, M. Brunsting, K. C. Tam, *Chem. Eng. J.* **2020**, *392*, 124821, https://doi.org/10.1016/j.cej.2020.124821.

[7] H. Yu, S. Oh, Y. Han, S. Lee, H. S. Jeong, H.-J. Hong, *Chemosphere* **2021**, *285,* 131448, https://doi.org/10.1016/j.chemosphere.2021.131448.

[8] J. Mao, J. Iocozzia, J. Huang, K. Meng, Y. Lai, Z. Lin, *Energy Environ. Sci.* **2018**, *11,* 772, https://doi.org/10.1039/C7EE03031B.

[9] J. Chen, T. Zhang, W. Hua, P. Li, X. Wang, *Colloid Surf., A* **2020**, *585,* 124048, https://doi.org/10.1016/j.colsurfa.2019.124048.

[10] S. V. Vadanan, A. Basu, S. Lim, *Polym. J.* **2022**, *54,* 481, https://doi.org/10.1038/s41428-021-00606-8.

[11] A. Kramar, F. J. González-Benito, *Polymers* **2022**, *14,* 286, https://doi.org/10.3390/polym14020286.

[12] H. P. S. Abdul Khalil, A. S. Adnan, E. B. Yahya, N. G. Olaiya, S. Safrida, Md. S. Hossain, V. Balakrishnan, D. A. Gopakumar, C. K. Abdullah, A. A. Oyekanmi, D. Pasquini, *Polymers* **2020**, *12,* 1759, https://doi.org/10.3390/polym12081759.

[13] F. Deuber, S. Mousavi, L. Federer, M. Hofer, C. Adlhart, *ACS Appl. Mater. Interfaces* **2018**, *10,* 9069, https://doi.org/10.1021/acsami.8b00455.

[14] F. Deuber, S. Mousavi, M. Hofer, C. Adlhart, *ChemistrySelect* **2016**, *1,* 5595, https://doi.org/10.1002/slct.201601084.

[15] S. Zhang, Q. Fan, Y. Pan, W. Wang, R. Lin, G. Chen, *Drying Technol.* **2024**, *42,* 1119, https://doi.org/10.1080/07373937.2023.2295531.

[16] G. Mol, C. Fialová, C. Adlhart, *Mater. Adv.* **2024**, *5,* 3929, https://doi.org/10.1039/D3MA00781B.

[17] F. Deuber, C. Adlhart, *CHIMIA* **2017**, *71,* 236, https://doi.org/10.2533/chimia.2017.236.

[18] L.-Y. Long, Y.-X. Weng, Y.-Z. Wang, *Polymers* **2018**, *10,* 623, https://doi.org/10.3390/polym10060623.

[19] S. Gupta, F. Martoïa, L. Orgéas, P. Dumont, *Appl. Sci.* **2018**, *8,* 2463, https://doi.org/10.3390/app8122463.

[20] P. Risch, C. Adlhart, *CHIMIA* **2022**, *76,* 354, https://doi.org/10.2533/chimia.2022.354.

[21] F. Martoïa, T. Cochereau, P. J. J. Dumont, L. Orgéas, M. Terrien, M. N. Belgacem, *Mater. Des.* **2016**, *104,* 376, https://doi.org/10.1016/j.matdes.2016.04.088.

[22] S. Pinches, G. V. Franks, *J. Am. Ceram. Soc.* **2023**, *106,* 5167, https://doi.org/10.1111/jace.19149.

[23] A. Du, M. Liu, S. Huang, C. Li, B. Zhou, *Molecules* **2018**, *23,* 1522, https://doi.org/10.3390/molecules23071522.

[24] S. Deville, 'Freezing Colloids: Observations, Principles, Control, and Use: Applications in Materials Science, Life Science, Earth Science, Food Science, and Engineering', Springer International Publishing, Cham, **2017**, https://doi.org/10.1007/978-3-319-50515-2.

[25] C. Cai, Z. Wei, C. Ding, B. Sun, W. Chen, C. Gerhard, E. Nimerovsky, Y. Fu, K. Zhang, *Nano Lett.* **2022**, *22,* 4106, https://doi.org/10.1021/acs.nanolett.2c00844.

[26] M. Yan, Y. Pan, X. Cheng, Z. Zhang, Y. Deng, Z. Lun, L. Gong, M. Gao, H. Zhang, *ACS Appl. Mater. Interfaces* **2021**, *13,* 27458, https://doi.org/10.1021/acsami.1c05334.

[27] Q. Liu, Y. Liu, Q. Feng, C. Chen, Z. Xu, *J. Hazard. Mater.* **2023**, *441,* 129965, https://doi.org/10.1016/j.jhazmat.2022.129965.

[28] C. Jiménez-Saelices, B. Seantier, B. Cathala, Y. Grohens, *J. Sol-Gel Sci. Technol.* **2017**, *84,* 475, https://doi.org/10.1007/s10971-017-4451-7.

[29] S. Zhang, Y. Pan, W. Wang, R. Lin, X. Liu, *Ind. Crops Prod.* **2023**, *194,* 116303, https://doi.org/10.1016/j.indcrop.2023.116303.

[30] S. Zhao, W. J. Malfait, N. Guerrero-Alburquerque, M. M. Koebel, G. Nyström, *Angew. Chem. Int. Ed.* **2018**, *57,* 7580, https://doi.org/10.1002/anie.201709014.

[31] N. Reddy, R. Reddy, Q. Jiang, *Trends Biotechnol.* **2015**, *33,* 362, https://doi.org/10.1016/j.tibtech.2015.03.008.

[32] S. Mousavi, L. Filipová, J. Ebert, F. J. Heiligtag, R. Daumke, W. Loser, B. Ledergerber, B. Frank, C. Adlhart, *Sep. Purif. Technol.* **2022**, *284,* 120273, https://doi.org/10.1016/j.seppur.2021.120273.

[33] Y. Shen, D. Li, B. Deng, Q. Liu, H. Liu, T. Wu, *R. Soc. Open Sci.* **2019**, *6,* 190596, https://doi.org/10.1098/rsos.190596.

[34] C. Wang, H. Cao, L. Jia, W. Liu, P. Liu, *Carbohydr. Polym.* **2022**, *291,* 119568, https://doi.org/10.1016/j.carbpol.2022.119568.

[35] Y. Chen, D. Fan, S. Lyu, G. Li, F. Jiang, S. Wang, *ACS Sustainable Chem. Eng.* **2019**, *7,* 1381, https://doi.org/10.1021/acssuschemeng.8b05085.

[36] J. Zhuang, M. Pan, Y. Zhang, F. Liu, Z. Xu, *Int. J. Biol. Macromol.* **2023**, *235,* 123884, https://doi.org/10.1016/j.ijbiomac.2023.123884.

[37] Y. Li, N. Grishkewich, L. Liu, C. Wang, K. C. Tam, S. Liu, Z. Mao, X. Sui, *Chem. Eng. J.* **2019**, *366*, 531, https://doi.org/10.1016/j.cej.2019.02.111.

[38] F. Jiang, Y.-L. Hsieh, *Appl. Mater. Interfaces* **2017**, *9,* 2825, https://doi.org/10.1021/acsami.6b13577.
[39] H. Fang, N. Feng, D. Wu, D. Hu, *Biomacromol.* **2021**, *22,* 4155, https://doi.org/10.1021/acs.biomac.1c00650.
[40] L. J. Gibson, M. F. Ashby, 'Cellular Solids: Structure and Properties', Cambridge University Press, **1997**, https://doi.org/10.1017/CBO9781139878326.
[41] K. Ganesan, A. Barowski, L. Ratke, *Molecules* **2019**, *24,* 2688, https://doi.org/10.3390/molecules24152688.
[42] S. Sepahvand, M. Jonoobi, A. Ashori, D. Rabie, F. Gauvin, H. J. H. Brouwers, Q. Yu, T. H. Mekonnen, *Int. J. Biol. Macromol.* **2022**, *203,* 601, https://doi.org/10.1016/j.ijbiomac.2022.01.156.

License and Terms

The definitive version of this article is the electronic one that can be found at https://doi.org/10.2533/chimia.2025.232